한국측지학회지, 제 12 권, 제 1 호, pp.95~106(1994년 6월 30일)

The Global Geopotential Models in the Region of Korean Peninsula

Yun, Hong-Sic* · Jozsef Adam**

ABSTRACT

The purpose of this paper is to establish the optimum reference field as testing some geopotential model, gravity data and GPS data. We have to decide a best fitting geopotential model as a reference surface for establishing the optimum geoid solutions. We conduct some tests on the Korean Peninsula gravity data to establish which of the model would be prove to be the best one. Three ways were used to compare the geopotential coefficient solutions. One of the tests is to compare the residual gravity anomaly remaining after the anomaly computed from the geopotential model has been subtracted from the "observed" gravity anomaly. The second method is a comparison of several geopotential solutions in terms of differences in gravity anomalies and quasi-geoid undulations. The third method is a comparison between the undulation obtained by GPS and the corresponding undulation from each geopotential model. The result showed that OSU91A model is a best fitting model as a reference in the region of Korean Peninsula.

要　　旨

지오이드 모델링에 필요한 기준면으로 사용되는 여러가지 지오포텐셜모델들을 시험하여 한반도 주변의 최적기준면을 결정하고자 하였다. 시험은 지오포텐셜모델들로부터 계산된 중력이상과 실제측정한 중력이상의 차를 검토하였으며, 지오포텐셜모델들간의 중력이상과 지오이드고의 차를 비교·검토하였다. 또한 GPS 측량데이타로부터 계산된 지오이드고와 지오포텐셜모델로부터 계산된 지오이드고를 검토하였다. 시험결과 OSU91A 모델이 한반도 주변에서의 기준면으로 적합하다는 것을 알 수 있었다.

1. Introduction

Modern trend in Geodesy demand an increased accuracy of relative heights and height changes. Due to such a requirement, we have to be made the unique height determination by taking into account the convergence and irregulaties of the equipotential surfaces of the earth's actural gravity field.

The height of a point on the terrestrial surface is usually defined as the distance between an equipotential surface through the point in question and the corresponding equi-potential surface representing the height datum, measured along the line of force or along its tangent.[17]

The three dimensional geodesy has been practically split into two parts, horizontal and vertical coordinates, and treated separately. The height datum known as the orthometric height used in vertical coordinate has been chosen to be the geoid. The geoid defined as a particular equi-potential surface of the earth's actual gravity field the undisturbed mean sea level can be determined by using several data sets such as earth's gravity potential, terrestrial gravity measurement data, digital terrain

*PhD Student, Department of geodesy, Technical University of Budapest
**Professor, Department of geodesy, Technical University of Budapest

Table 1. Some Currently used Global Geopotential Models

Field	Auther	Date	Nmax
GEM10B	Lerch, F.J. et al	1981	36
GEM10C	Lerch, F.J. et al.	1981	180
OSU81	Rapp, R.H.	1981	180
GPM2	Wenzel, H.-G.	1985	200
GEMT1	Marsh, J.G. et al.	1988	36
GEMT2	Marsh, J.G. et al.	1989	50
GEMT3	Marsh, J.G. et al.	1993	50
IFE87E1	Basic, T.	1989	200
IFE88E1	Basic, T.	1989	360
OSU86E	Rapp, R.H. and J.Y. Cruz	1986	360
OSU86F	Rapp, R.H. and J.Y. Cruz	1986	360
OSU89A	Rapp, R.H. and N.K. Pavlis	1989	360
OSU89B	Rapp, R.H. and N.K. Pavlis	1989	360
OSU91A	Rapp, R.H. and	1991	360
TEG2/3	B.D. Tapley, C.K. Shum, et al.	1993	70
GRIM4	R. Biancale, G, Balmino, et al.	1993	60

model, deflection of vertical, doppler data, and GPS data etc.

Recently geodesy has witnessed a renaissance in the geoid computation. The advances over the past decades have taken place at all wavelength, and have brought forth major improvements in accuracy.[8)]

The examples of long-wavelength global gravitational models are the GEMT1,2,3 (Goddard Earth Model: GEM) solutions which are complete to degree and order 36, incomplete to degree and order 50 and the short-wavelength global models term high degree are shown in Table 1.

The geopotential models shown in Table 1 have a number of different applications in the geodetic science and practice for the calculation of reference models for gravimetric predictions, calculation of gravimetric quantities (N, Δg) on a point by point, basic model simulation studies involving future gravity field missions, study of the global spectra of the Earth's gravity field, calculation of gravimetric quantities at satellite altitude, geophysical investigations of the earth's interior, and oceanographic studies related to ocean dynamics etc.[5)]

In Table 1 GEMT1, GEMT2 and GEMT3 are examples of satellite-alone solutions which are derived from satellite observations only. They contain harmonics up to degree and order 36 and 50, and contain 1406 and 2028 coefficients.

Other global geopotential models are obtained by using terrestrial gravimetry, altimetry and DTM data, and they normally contain more coefficients.

Examples of these models are the OSU81, GPM2, and OSU86E/F, OSU89A/B and OSU91A which contain harmonics up to degree 180, 200, 360 and contain 32942, 40602 and 13068 coefficients respectively. The more coefficients there are in a model, the more precise model is because it contains shortest wavelength informations of the earth's gravity field. The latest high degree global geopotential model is the OSU91A model complete to n,m=360, which were developed through the combinations of GEMT1, 2 coefficients set, Geos 3/Seasat altimeter derived anomalies and the latest terrestrial gravity data base.

Recently as a new geopotential model, the TEG-3 Geopotential Model is complete up to degree and order 70 in spherical harmonics. The TEG-3 model is a complete iteration of the data in TEG-2 series model, with improved force and measurement modelling, and using additional data, including the Spot-2 Doris data, Topex/Poseidon laser and Doris data, ERS-1 laser and altimeter data, Topex/Poseidon Demo global Positioning System (GPS) tracking data and altimeter data, and laser tracking data from Lageos-2, Etalon-1 and Etalon-2.[7)]

The GRIM4 generation of earth gravity field models initiated in 1990 with the GRIM S1/C1 models is now completed with the GRIM4 S4/C4 models. It contains the shperical harmonic expansion which is complete up to degree and order 60 included satellite data from Lageos, Spot2 and altimetry satellites ERS1 and Topex/Poseidon and also combined model C4 with respect to the OSU87 data set of new gravimetric data from the BGI data base over Asia and South America, and the use of the OSU92 marine geoid. The new GRIM4 models realize a better adequation in ERS1 and Topex/Poseidon orbit adjustment.[7)] The total geoid error to be expected from the use of OSU91A to degree 360 is $\pm$ 50 cm.[25)]

The purpose of this paper is to compare some

geopotential models to determine the optimum reference field in Korean Peninsula. The potential coefficient solutions can be compared in many ways[8,9] some of which will be applied here as follows;

(1) we can be evaluated the statistics of residual gravity anomaly δg(i) using the formula,

$$\delta g(i) = \Delta g(i) - \Delta g^*(i) \quad (1)$$

where

Δg(i) is the free air anomaly generated from the 'observed' gravity.

Δg*(i) is the gravity anomaly generated from the geopotential model.

In other words, equation (1) means that the smaller the residual gravity field, the more precise geoid heights derived from the geopotential model.

For this test Δg*(i) were generated on 1165 points in the region of Korean Peninsula using some selected geopotential models in Table 1. A value of Δg*(i) was computed at each gravity point in used data set provided by BGI as shown in Fig. 1, and δg(i) were obtained by equation (1). The δg(i) were then analysed to obtain the mean and standard deviation for the population.

(2) The differences in gravity anomalies and undulation between different geopotential solutions can be statitically analyzed. For the generation of the reference gravity anomalies and geoid undulations from the geopotential model coefficients, the efficient algorithm of Rizos has been used.

(3) The geopotential fields can be evaluated through comparison of GPS points quasigeoid undulations (ζ_{GPS}) with undulations from various geopotential models (ζ_{GOP}) by

$$\delta\zeta(i) = \zeta_{GPS}(i) - \zeta_{GOP}(i) \quad (2)$$

This can only be done after when GPS coordinates have been converted to a geocentric, true scale system. The accuracy of a geopotential coefficient model may also be evaluated by this way.

2. Computation and Discussion

In here we have been evaluated several geopotential models selected in Table 1 using by the above mensioned three methods. A number of tests have been carried out on the ablility of geopotential model to represent the gravity field in the region of Korean Peninsual in order to establish their values as a reference field for geoid soultions. We also have compared some high degree solutions againt each other for interest.

2.1 Computing Geoid Undulation and Anomalies from Geopotential Model

An earth geopotential model is available with coefficients C_{nm} and S_{nm} complete up to degree and order n,m. Then the reference undulation (e.g. the long wavelength part of the geoid heights) and the gravity anomalies are computed from the following truncated formula:

$$N = \frac{GM}{r\gamma} \sum_{n=0}^{n} \left[\frac{a}{r}\right]^n \sum_{m=0}^{n} \quad (3)$$

$$[\bar{C}_{nm} \cos m\lambda + \bar{S}_{nm} \sin m\lambda] \bar{P}_{nm}(\sin\phi)$$

$$\Delta g = \gamma \sum_{n=2}^{n=n_{max}} (n-1) \sum_{m=0}^{n} [(\bar{C}_{nm} - \bar{C}'_{no}) \quad (4)$$

$$\cos m\lambda + \bar{S}_{nm} \sin m\lambda] \bar{P}_{nm}(\cos\phi)$$

$$N = R \sum_{n=2}^{n=n_{max}} \sum_{m=0}^{n} [(\bar{C}_{nm} - \bar{C}'_{no}) \cos m\lambda \quad (5)$$

$$+ \bar{S}_{nm} \sin m\lambda] \bar{P}_{nm}(\sin\phi)$$

where

C_{nm}, S_{nm} are the fully normalized geopotential coefficients

C'_{no} is the coefficients of the normal reference field

P_{nm} is the fully normalized Legendre functions

n_{max} is the maximum degree of the geopotential model (360)

γ is the mean gravity

R is the mean radius of the earth

ϕ is the geocentric latitute

Undulations computed in this way have an estimated absolute accuracy of about 0.5 m.

2.2 Comparison of the Residual Gravity Anomalies

The test of the fit of high order geopotential mo-

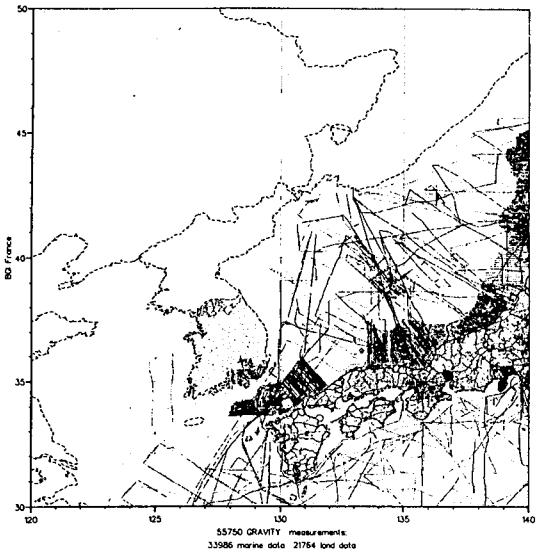

Fig. 1. Distribution of Gravity Data Provided by BGI

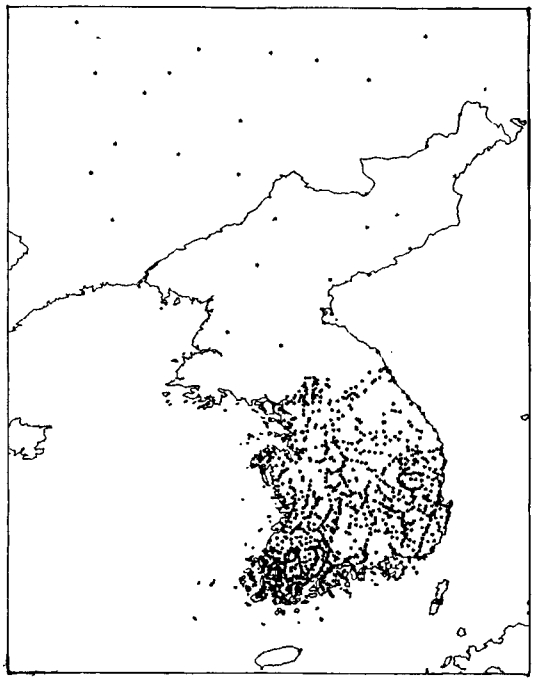

Fig. 2. Distribution of Graivty Data used in Test Computation

dels to the gravity field in Korean Peninsula is based on using the point gravity data. Fig. 2 shows the location of the used gravity data in this test. We have transformed this data sets into the GRS80 and IGSN system for comparing with the geopotential solutions, after than computed the gravity anomalies using equation (4) and (5), and compared to the gravity data by calculation of residual gravity anomalies by equation (1).

Some of the global geopotential solutions presented in Table 1 are used for comparison with each other. The best "fitness" of the models by computing a reference gravity anomalies and comparing them to terrestrial gravity anomalies over the Korean Peninsula has been investigated. The results are summariezed in the following Table 2.

The results of this table show that the ability of high order geopotential models to model the geoid and terrsstrial gravity varies according to the model used, the degree and order of the model and the bahaviour of the quasigeoid in the region in which the computation was done. The result also have been summarized to use some histograms as shown in Fig. 2, allowing a direct comparison between the models. We can see that all the geopotential model are able to recover gravity anomalies over 55% within 15 mgal and over 85% within 25

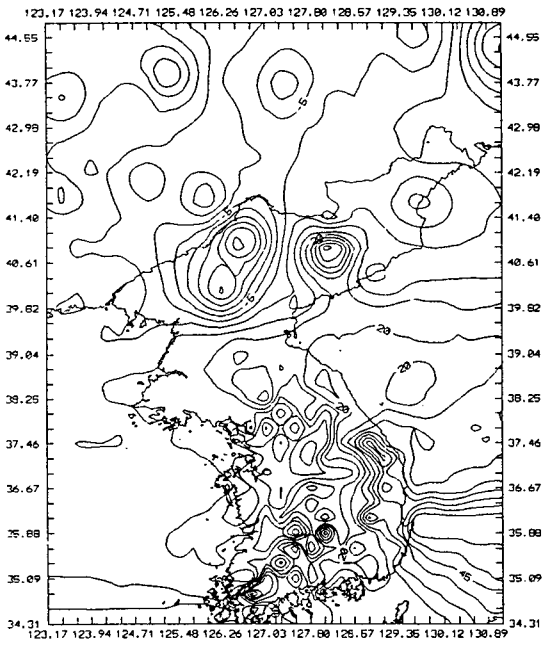

Fig. 3. Representation of the Free Air Anomalies

mgal of the region of Korean Peninsula. This test show that most of geopotential model are similar

Table 2. The Residual Gravity Anomalies

G.M. Model	Range of the Residual Gravity Anomalies in mGal (± 5 mgal) (%)						
	0−5	5−10	10−15	15−20	20−25	25−30	30<
GEMT1 − 36	237(20.3)	233(20.0)	221(19.0)	188(16.1)	145(12.4)	50(4.3)	91(7.8)
GEMT2 − 36	192(16.5)	214(18.4)	224(19.2)	190(16.3)	164(14.1)	87(7.5)	94(7.8)
GEMT2 − 50	196(17.0)	216(18.5)	221(19.0)	189(16.2)	160(14.0)	85(7.0)	98(8.4)
OSU86F −180	198(17.0)	221(19.0)	225(19.3)	188(16.1)	155(13.3)	82(7.0)	96(8.2)
−200	198(17.0)	222(19.0)	225(19.3)	189(16.2)	153(13.1)	82(7.0)	96(8.2)
−360	198(17.0)	220(18.9)	230(20.0)	189(16.2)	150(12.9)	82(7.0)	96(8.2)
OSU89A −180	196(16.8)	217(18.6)	218(18.7)	192(16.5)	157(13.5)	86(7.4)	82(7.0)
−200	198(17.0)	215(18.5)	221(19.0)	191(16.4)	156(13.4)	86(7.4)	98(8.4)
−360	197(17.0)	220(19.0)	222(19.0)	189(16.2)	153(13.0)	86(7.4)	98(8.4)
OSU89B −180	198(17.0)	221(19.0)	225(19.3)	188(16.1)	155(13.3)	82(7.0)	96(8.2)
−200	198(17.0)	222(19.0)	225(19.3)	189(16.2)	153(13.1)	82(7.0)	96(8.2)
−360	198(17.0)	220(18.9)	230(20.0)	189(16.2)	150(12.9)	82(7.0)	96(8.2)
OSU91A −180	196(16.8)	215(18.5)	228(19.6)	188(16.1)	159(13.6)	85(7.3)	94(8.1)
−200	198(17.0)	216(18.5)	224(19.2)	191(16.4)	159(13.6)	84(7.3)	93(8.0)
−360	195(16.7)	217(18.6)	231(19.8)	184(15.8)	160(13.7)	85(7.3)	93(8.0)
GPM2 −180	199(17.1)	223(19.1)	222(19.1)	196(16.8)	152(13.0)	79(6.8)	94(8.1)
−200	200(17.2)	223(19.1)	222(19.1)	203(17.4)	143(12.3)	81(7.0)	93(8.0)
IFE87E −180	199(17.1)	220(18.9)	222(19.1)	197(16.9)	153(13.1)	79(6.8)	95(8.2)
−200	201(17.3)	221(19.0)	220(18.9)	203(17.4)	146(12.5)	80(6.9)	94(8.1)

to each other and have no big difference when we consided the degree and order. Table 3 shows the statistics of the residual gravity anomalies. The mean value and standard deviation are small in the case of OSU91A models. Fig. 3 is presented the residual gravity anomalies based on each model up to degree and order 50, 200, 360.

The result of this comparison show that the OSU 86F, OSU89B and OSU91A model describes the quasigeoid most closely in Korean Peninsula. These model up to degree and order 360 fits the gravity anomaly field of Korean Peninsula in the same measure or better than the other geopotential models.

2.3 Comparison of Standard Deviations

The next set of comparison is to indicate the regional, standard deviation, geoid undulation and gravity anomaly differences between several solutions. The geoid undulations (height anomalies) and gravity anomaly difference were computed with a direct evaluation on a gravity point within the area [125°<ϕ<129°; 33°<λ<45°] involving Korean Peninsula. A total of 1165 points for geoid undulations

Table 3. The Statistics of the Residual Gravity Anomalies

Geopotential Model	Statistics of the Residual Gravity Anomalies [mGal]			
	Mean	Std. Dev.	Min.	Max.
GEMT1 − 36	−7.16	17.23	−96.21	105.51
GEMT2 − 36	−9.63	16.98	−98.92	102.16
− 50	−9.55	17.04	−98.90	102.48
OSU86F −180	−9.30	17.02	−98.69	102.04
−200	−9.30	17.02	−98.69	102.03
−360	−9.30	16.95	−98.78	102.09
OSU89A −180	−9.60	17.01	−98.87	101.67
−200	−9.59	17.01	−99.01	101.72
−360	−9.61	16.95	−99.11	101.78
OSU89B −180	−9.30	17.02	−98.58	101.94
−200	−9.30	17.02	−98.69	102.03
−360	−9.30	16.95	−98.78	102.09
OSU91A −180	−9.35	17.04	−98.77	102.43
−200	−9.35	17.04	−98.86	102.43
−360	−9.36	16.98	−98.99	102.14
GPM2 −180	−8.98	17.04	−98.27	103.19
−200	−8.96	17.01	−98.37	102.85
IFE87E1 −180	−9.06	17.04	−98.35	103.13
−200	−9.08	17.01	−98.46	102.78

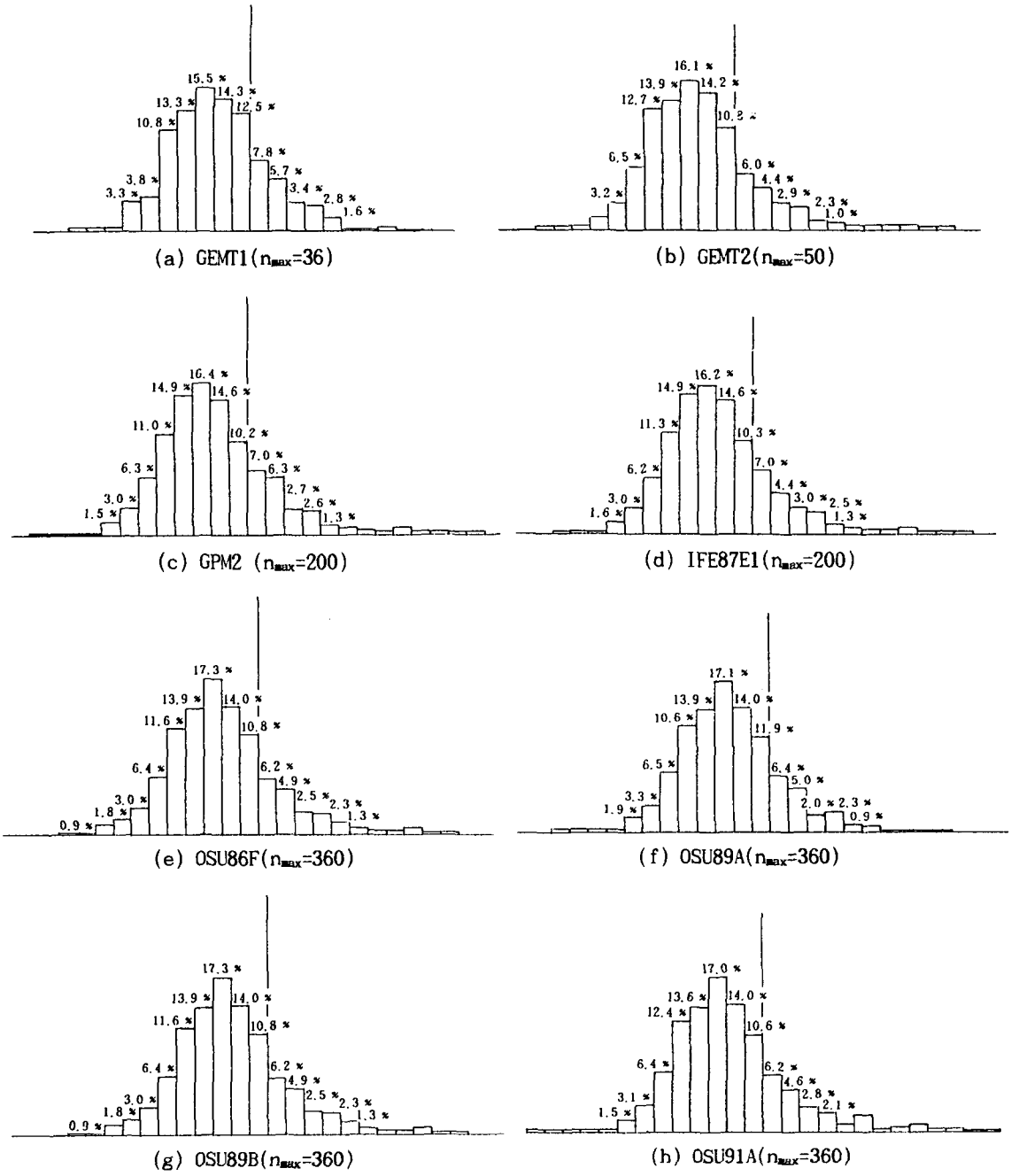

Fig. 4. Distribution of Residual of Geopotential Model minus Observed Point Values of Δg [mGal]

and gravity anomalies were computed. Differences in gravity anomalies and undulations between geopotential solutions computed by equation (1) and (2) were statitically analysed. The results of these comparisons are summarized in Table 4.

Although the difference between different solutions is small there are large discrepancies that reach some tens of magls in gravity anomalies and undulations are −63.64 mgal and 59.66 mgal, −4.78 m and 4.78 m in this regional area respecti-

Table 4. Geopotential coefficient Difference in terms of Gravity Anomalies (mgal) and Geoid Undulation (m)

Geopotential Solution		Δg [mGal]				N [m]			
		Mean	S.T.	Min.	Max.	Mean	S.T.	Min.	Max.
[360]									
OSU91A	− OSU89B	−1.05	2.76	−11.43	29.62	−0.24	0.48	−1.64	3.14
	− OSU89A	−0.18	3.26	−23.61	39.97	−0.24	0.48	−1.64	3.14
	− OSU86F	1.05	2.76	−11.43	29.62	0.58	0.48	−1.85	1.89
OSU89B	− OSU89A	−1.24	2.79	−23.03	51.40	−0.30	0.27	−1.45	4.32
	− OSU86F	0	0	0	0	0	0	0	0
OSU89A	− OSU86F	1.24	2.79	−51.40	23.03	0.30	0.27	−4.32	1.45
[200]									
OSU91A	− OSU89B	0.92	2.45	−11.36	16.45	0.05	0.48	−1.89	1.68
	− OSU89A	−0.18	3.32	−16.56	48.30	−0.24	0.48	−1.74	3.46
	− OSU86F	0.92	2.45	−11.36	16.45	0.05	0.48	−1.89	1.68
	− GPM 2	3.87	9.07	−47.98	19.07	0.36	0.54	−2.59	1.02
	− IEF87E1	3.75	8.95	−47.50	18.52	0.27	0.54	−2.66	0.92
OSU89B	− OSU89A	−1.10	2.86	−13.77	59.66	−0.30	0.29	−1.44	4.78
	− OSU86F	0	0	0	0	0	0	0	0
	− GPM 2	2.95	8.70	−42.81	19.49	0.31	0.51	−2.09	1.67
	− IFE87E1	2.83	8.59	−42.33	18.81	0.22	0.51	−2.24	1.59
OSU89A	− OSU86F	1.10	2.86	−59.66	13.77	0.30	0.29	−4.78	1.28
	− GPM 2	4.04	8.88	−62.83	21.28	0.61	0.55	−4.32	1.59
	− IFE87E1	3.92	8.79	−62.42	20.83	0.52	0.55	−4.43	1.50
OSU86F	− GPM 2	2.95	8.70	−42.81	19.49	0.31	0.51	−2.09	1.67
	− IFE87E1	2.83	8.59	−42.33	18.81	0.22	0.51	−2.24	1.59
GPM 2	− IFE87E1	−0.12	0.35	−1.42	1.59	−0.09	0.01	−0.16	−0.05
[180]									
OSU91A	− OSU89B	0.78	2.25	−10.98	14.24	0.05	0.47	−1.91	1.61
	− OSU89A	−0.39	3.07	−16.80	46.49	−0.25	0.47	−1.61	3.41
	− OSU86F	0.78	2.25	−10.98	14.24	0.05	0.47	−1.91	1.61
	− GPM 2	4.29	7.97	−33.37	21.06	0.37	0.51	−2.14	1.06
	− IEF87E1	4.15	7.39	−30.53	19.51	0.28	0.51	−2.17	0.99
OSU89B	− OSU89A	−1.17	2.92	−57.47	14.21	0.30	0.29	−4.71	1.43
	− OSU86F	0	0	0	0	0	0	0	0
	− GPM 2	3.38	7.21	−26.28	19.99	0.32	0.49	−2.02	1.61
	− IFE87E1	3.37	7.19	−26.82	20.08	0.24	0.49	−2.21	1.53
OSU89A	− OSU86F	1.17	2.92	−57.47	14.21	0.30	0.29	−4.71	1.43
	− GPM 2	4.55	7.70	−63.32	22.60	0.62	0.53	−4.35	1.72
	− IFE87E1	4.54	7.67	−63.64	22.24	0.54	0.53	−4.45	1.63
OSU86F	− GPM 2	3.38	7.21	−26.28	19.99	0.32	0.49	−2.02	1.61
	− IFE87E1	3.37	7.19	−26.82	20.08	0.24	0.49	−2.21	1.53
GPM 2	− IFE87E1	−0.01	0.28	−1.15	0.91	−0.09	0.01	−0.15	−0.06
[36]									
GEMT2	− GEMT1	26.72	2.51	9.54	30.90	23.31	2.41	11.00	26.79

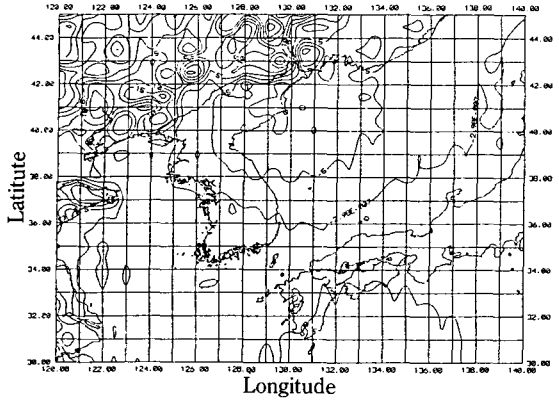

Fig. 5. Gravity Anomaly Differences: OSU91A minus OSU89B complete degree and order 360. The contour interval is 5 mgal

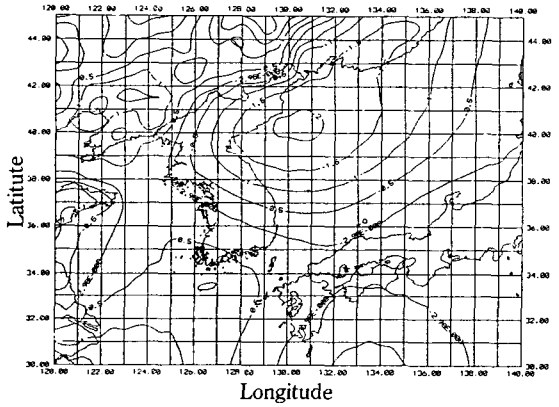

Fig. 6. Geoid Undulation Differences: OSU91A minus OSU89B complete degree and order 360. The contour interval is 0.5 m

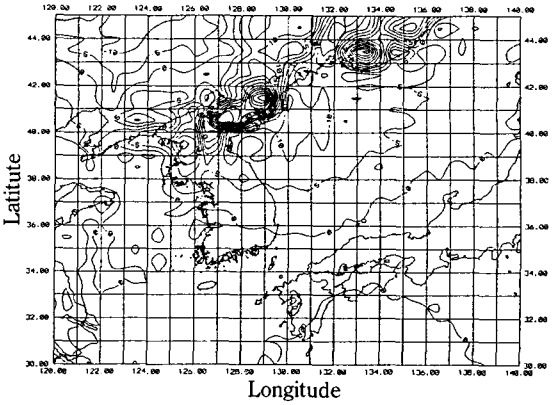

Fig. 7. Gravity Anomaly Differences: OSU91A minus OSU89A complete degree and order 360. The contour interval is 5 mgal

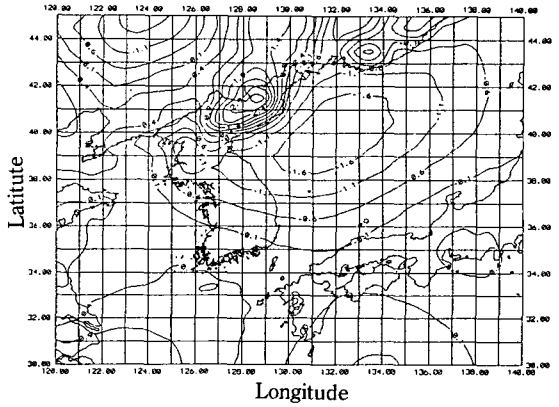

Fig. 8. Geoid Undulation Differences: OSU91A minus OSU89A complete degree and order 360. The contour interval is 0.5 m

vely.

In order to obtain more informations we have plotted regional undulation and anomaly difference maps between geopotential solutions. These maps were made by contouring data grided at a 0.25°× 0.25° interval.

In Fig. 5 through 12 the gravity anomaly and undulation difference between OSU91A, OSU89A, OSU89B and OSU86F are illustrated.

Large systematic discrepancies occur in the northern parts within the investigated area having a maximum and minimum difference of 60 mgal and −10 mgal in gravity anomalies and of −0.6 m and 3.0 m in undulations in compared with OSU89A model. This difference in the northern part is due to OSU89A model which does not considered the topographic effect. Fig. (7) through (12) we have seen that the topographic effect is quite large in a case of which is not contained a terrestrial gravity data in geopotential models.

Fig. 7, 9, 11 shows a map of gravity anomaly difference between the OSU91A, OSU89A and OSU 89B, OSU86F solution with large discrepancies noted. A similar map is shown in Fig. 8, 10, 12 for the undulation differences between each solutions. Incresing systematic discrepancies between these solutions are seen by going from the southern part to the northern part of Korean Peninsula.

The gravity anomalies and quasigeoid undulations of OSU91A and OSU89A for the Korean Peni-

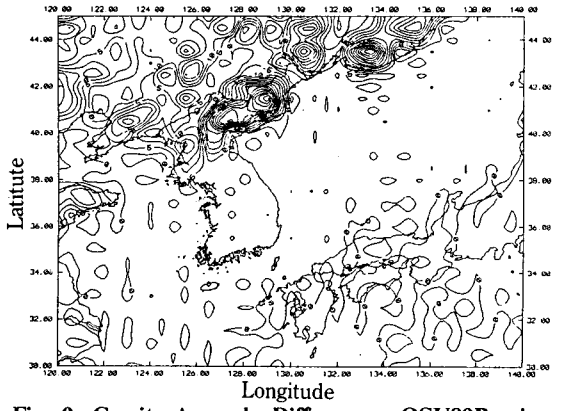

Fig. 9. Gravity Anomaly Differences: OSU89B minus OSU89A complete degree and order 360. The contour interval is 5 mgal

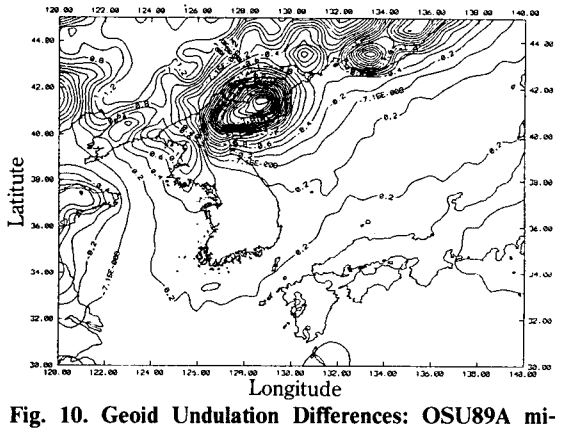

Fig. 10. Geoid Undulation Differences: OSU89A minus OSU89B complete degree and order 360. The contour interval is 0.5 m

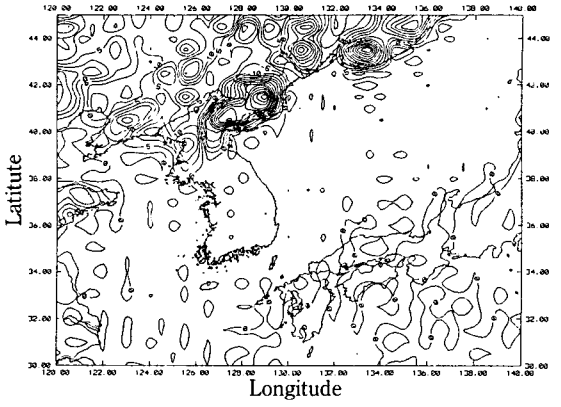

Fig. 11. Gravity Anomaly Differences: OSU89A minus OSU86F complete degree and order 360. The contour interval is 5 mgal

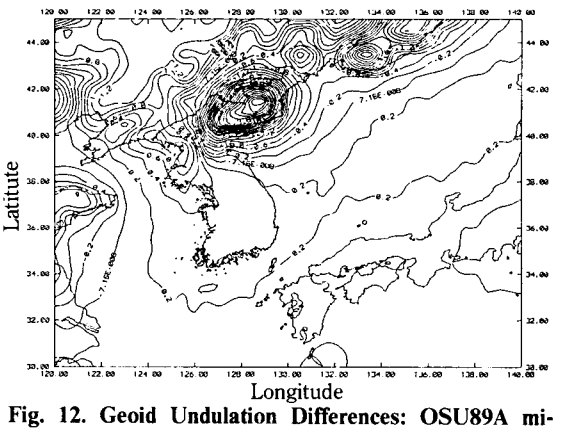

Fig. 12. Geoid Undulation Differences: OSU89A minus OSU86F complete degree and order 360. The contour interval is 0.5 m

nsula in GRS80 system is shown in Fig. 13, 14, 15 and 16 respectively. The quasigeoid undulation of the above OSU geopotential models complete up to degree and order 360 referring to GRS80 around the Korean Peninsula range from 20.0 m to 30.0 m (Fig. 14, 16). This tests show that the OSU89B model is the same as OSU86F model exactly in the region of Korean Peninsula.

2.4 Comparison of GPS and Geopotential Models

We turn to a comparison of the quasigeoid undulations derived from the various geopotential models with undulations derived from GPS positions. In all comparisons, I used 25 points from some papers including a few points which converted from GPS postion to a local geodetic system by P.H. Park, et all.,.

The comparisons have been carried out with the GEMT1, 2, OSU86F, OSU89A/B and OSU91A, GPM 2 and IFE87E1 models.

$$N = h - H \tag{6}$$

First we are computed the geoid undulation from GPS data by equation (6) as shown in Table 5.

The mean difference (GPS minus Model) and standard deviation of the difference is given in Table 6. The mean value and standard deviation

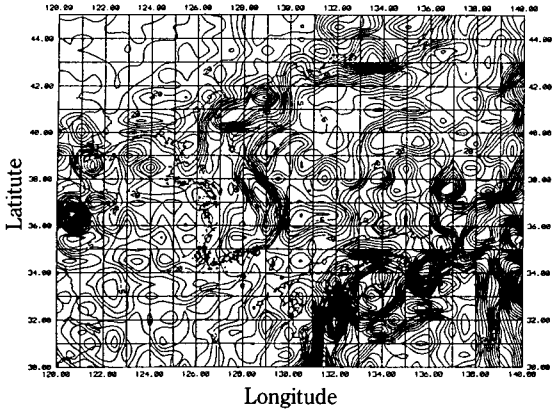

Fig. 13. Gravity Anomaly: OSU91A complete degree and order 360. The contour interval is 5 mgal

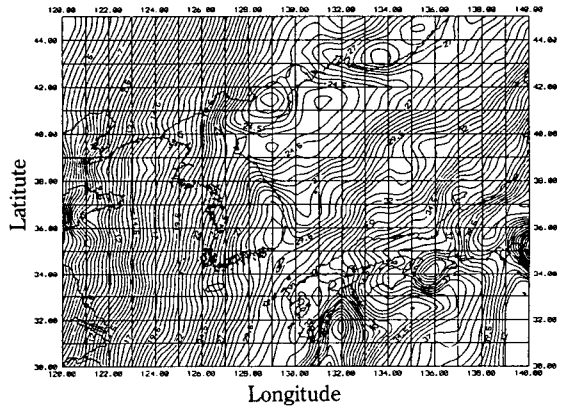

Fig. 14. Geoid Undulation: OSU91A complete degree and order 360. The contour interval is 0.5 m

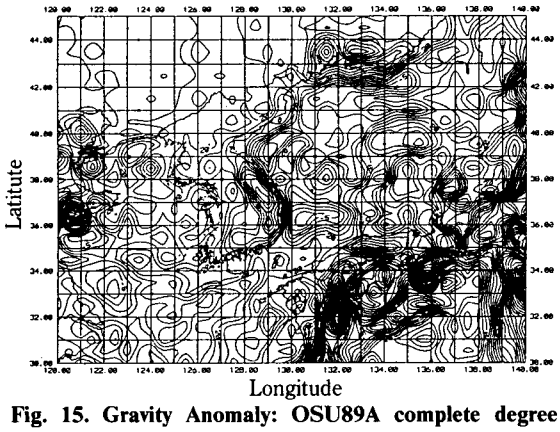

Fig. 15. Gravity Anomaly: OSU89A complete degree and order 360. The contour interval is 5 mgal

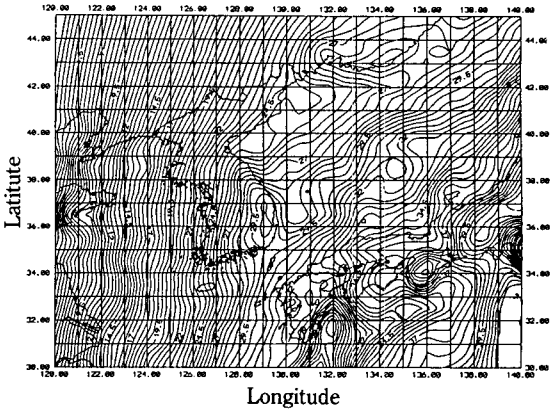

Fig. 16. Geoid Undulation: OSU89A complete degree and order 360. The contour interval is 0.5 m

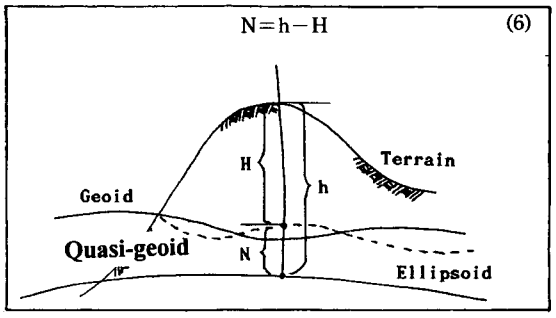

Fig. 17. The Quasi-Geoid Undulation

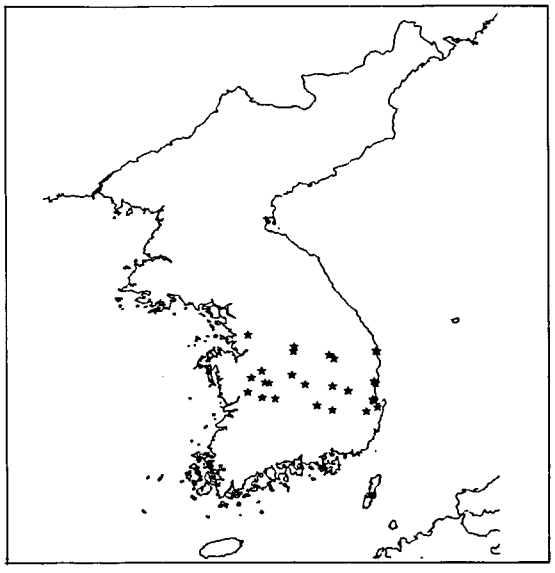

Fig. 18. Distribution of GPS Points

Table 5. Geoid Undulation computed from GPS and Geopotential Models

Points	Geoid Undulation (m)						
	(N=h−H)	O91A(360)	O89B(360)	O89A(360)	O86F(360)	GPM2(200)	IFE87(200)
1	25.498	25.37	25.42	25.76	25.42	24.54	24.62
2	25.288	26.09	26.09	26.40	26.09	25.39	25.47
3	25.391	26.76	26.64	26.97	26.64	26.21	26.28
4	25.027	24.90	24.85	25.20	24.85	24.28	24.35
5	25.392	25.95	25.80	26.14	25.80	25.49	25.56
6	24.598	24.99	24.83	25.19	24.83	24.60	24.66
7	26.460	27.01	27.15	27.47	27.15	26.36	26.45
8	29.165	29.61	29.70	30.00	29.70	29.16	29.23
9	27.816	29.54	29.71	29.98	29.71	28.95	29.03
10	29.800	29.71	29.85	30.15	29.85	29.14	29.21
11	27.435	27.70	27.76	28.09	27.76	27.38	27.48
12	26.118	26.34	26.74	27.06	26.74	25.83	25.94
13	32.004	28.82	29.43	29.71	29.43	28.21	28.28
14	28.012	28.53	28.48	28.80	28.48	28.15	28.25
15	29.751	29.38	29.67	29.94	29.67	28.95	29.02
16	27.934	28.51	28.95	29.24	28.95	27.93	28.01
17	28.244	28.84	28.98	29.27	28.98	28.57	28.66
18	29.580	30.00	30.03	30.32	30.03	29.18	29.25
19	26.561	26.47	26.82	27.15	26.82	25.89	25.99
20	28.901	28.86	29.47	29.75	29.47	28.22	28.29
21	29.656	29.31	29.28	29.57	29.28	28.63	28.72
22	29.555	29.39	29.70	29.97	29.70	28.93	29.01
23	28.578	28.74	29.16	29.45	29.16	28.16	28.24
24	29.411	29.60	29.77	30.04	29.77	28.98	29.06
25	29.573	29.75	29.90	30.19	29.90	29.14	29.21

Table 6. The Statistics of the Undulation between Qusi-Geoid and GPS derived geoid undulation

Geopotental Model		Mean	Std.Div.
GEMT1	− 36	2.690	1.039
GEMT2	− 36	−0.339	0.818
	− 50	−0.219	0.883
OSU86F	− 180	−0.292	0.868
	− 200	−0.260	0.871
	− 360	−0.337	0.770
OSU89A	− 180	−0.584	0.901
	− 200	−0.555	0.879
	− 360	−0.642	0.771
OSU89B	− 180	−0.292	0.868
	− 200	−0.260	0.871
	− 360	−0.337	0.770
OSU91A	− 180	−0.130	0.951
	− 200	−0.102	0.942
	− 360	−0.177	0.854
GPM2	− 180	0.435	0.920
	− 200	0.379	0.881
IFE87E1	− 180	0.331	0.928
	− 200	0.299	0.883

agreement between GPS and models reaches −0.102 m, 2.690 m and 0.770 m, 1,039 m respectively. As we consider mean value and standard deviation simultaneously, we can conclude that for Korean Peninsula, OSU91A model is better than the others. But most of high degree solutions are similar, and OSU89B and OSU86F solutions give the same results exactly.

3. Conclusions

Korea is in need of a precise quasigeoid, primarily to enable the use of GPS for surveying engineering (e.g. Levelling). In the local geoid (quasigeoid) determination we need a geopotential solution as the reference model. Therefore it is necessary to decide which model describes the geoid most closely in Korean Peninsula. An examination is presented to show that how well the gravity anomalies and quasigeoid undulations are able to be

recovered in Korean Peninsula using different high order global geopotential solutions. The results showed that OSU91A model is most suitable for use as a reference in the region of Korean Peninsula. However, large systematic discrepancies have been observed between different geopotential solutions in the northern part of Korea due to the shortage of terrestrial gravity data and topographic effect. We can conclude that (1) OSU91A model is better fit than the others as a reference in Korean Peninsula, (2) we have to considered the topographic effect in the region which has not sufficient terrestrial gravity data, (3) we need lots of GPS-derived undulation for determining the more accurate geoid surface.

Reference

1. A.H.W. Kearsely. Geoid Determination in the Philippines, School of Surveying, University of N.S.W, 1992.
2. A. Leick. GPS Satellite Surveying, 1990.
3. A. Tsen. Determination of Geoidal Height Difference using Ring Integration Method, UNB Technical Report, NO. 158, 1992.
4. Austrian Geodetic Commission. The Gravity Field in Austria, AGC Report, Graz, 1987.
5. FGI. Geodesy and Geophysics, Lecture Notes for NKG-Autumn School, Finland, 1992.
6. I.A. Tziavos. Numerical Considerations of FFT Methods in Gravity Field Modelling, Nr. 188, Hannover, 1993.
7. IAG General Meeting. Proceeding of IAG General Meetings, Peking, China, 1993.
8. J. Adam. Global Geopotential Models in the region of Hungary, XXth IUGG/IAG General Assembly, Vienna, Austria, 1991.
9. J. Adam et. al. Strategy for a New Hungarian Geoid Determination, 1988.
10. J. Adam. Status of the Geoid Determination in Hungary.
11. J. Adam. Geoid Activities in Hungary from Beginning up to 1991.
12. J. Adam and H. Denker. Test Computation for a Local Quasigeoid in Hungary using FFT, Acta Geodet., Geophys. et Montainist, Hungary, 1990.
13. J. Adam. On the consistency of the Coordinates of Station Penc Derived from Satellite Doppler Observation. Nablyudeniya ISZ, No 25, Budapest, 1987.
14. J. Adam. The Role of the Satellite Doppler Technique in the Improvement of the Geodetic Control Network in Hungary. Geodezia es Kartografia 39, 1987.
15. K. Kukums. Latvian Geoid Determination with Mass Point Frequency Domain Inversion, Reports of FGI, Helsinki, 1993.
16. M. Crespi, et. al. GPS Levelling and the Geoid, 2nd International Seminar on "GPS in Central Europe", Penc, Hungary, 1993.
17. M.M. Nassar. Gravity Field and Levelled Heights in Canada, UNB Technical Report No. 41, 1977.
18. M. Vermeer. Geoid Studies on Finland and Baltic, Reports of FGI, Helsinki, 1984.
19. M. Vermeer. A Fast Delivery GPS-Gravimetric Geoid for Estonoia, Reports of FGI, Helsinki, 1994.
20. P. Biro. On the Quasigeoid (in Hungray), EKME Tudomanyos Kozlemenyei, Vol. VIII, No. 2, Budapest, 1961.
21. P.H. Park, et. al. A Study on the Establishment of Geodetic Control Points for GPS, Journal of the Korean Society of Geodesy, Potogrammetry and Cartography, Vol 9, No. 1, 1991.
22. P.H. Park, J.U. Park, J.M. Kang. The Coordinate Transformation between Korean Geodetic System and WGS 84 for the Practical Use of GPS (I), Journal of the Korean Society of Geodesy, Potogra. and Carto., Vol 10, No. 1, 1992.
23. P.H. Park, J.U .Park, J.M. Kang. The Coordinate Transformation between Korean Geodetic System and WGS 84 for the Practical Use of GPS (II), Journal of the Korean Society of Geodesy, Potogra. and Carto., Vol 11, No. 1, 1993.
24. R.H. Rapp, N.K. Pavlis. The Development and Analysis of Geopotential Coefficient Models to Shperical Harmonic Degree 360, Journal of Geophysical Research Vol. 95, No. B13, 1990.
25. W. Bosch. A Rigorous Least Squares Combination of Low and High Degree spherical Harmonics, 1993.